

Modeling Hot Air Flow in the Trachea to Minimize Burn Damage

BEE 4530: Computer Aided Engineering: Applications to Biomedical Processes

Katharine Browning

James Chiang

Ankurita Datta

Sarah Modi

TABLE OF CONTENTS

1. Executive Summary.....	2
2. Introduction	
2.1 Background.....	3
2.2 Design Objectives.....	5
2.3 Model Design & Schematic.....	6
3. Results and Discussion	
3.1 Solution Analysis.....	10
3.2 Sensitivity Analysis.....	18
3.3 Accuracy Check.....	19
4. Conclusion	
4.1 Realistic Constraints.....	20
Appendix A: Mathematical Statement of the Problem.....	22
Appendix B: Solution Strategy.....	25
Appendix C: Additional Figures.....	28
Appendix D: References.....	29

1. EXECUTIVE SUMMARY

Thermal damage to the trachea causes respiratory problems. A few of these problems can cause difficulty breathing and can even lead to death. This damage typically occurs while breathing in abnormally hot air during fires. Treatment for tracheal burns is limited and frequently ineffective. Consequently, a better understanding of the relationship between inhaled air temperature and burn dynamics will help direct treatment plans for patients who experience this type of trauma. Additionally, comprehension of how different breathing cycles affect temperature and burning along the tracheal wall could help to reduce the amount of burning altogether.

To study these effects, we created a model of the trachea with hot air flow and analyzed how the temperature and burning changed as a function of inhalation temperature and velocity. Then, by varying the velocity and frequency of the breathing cycle, we determined how these parameters affect the extent of burn propagation throughout the trachea and the average amount of burn.

Our results show that tracheal burning was mostly limited to the proximal end and inner wall of the trachea with the temperature of the outer wall remaining unchanged over time. This is consistent with our expectations due to the geometry of the trachea. We also noted that there was no correlation between breathing frequency and volume of breath and the amount of burn that the tissue sustained. This result contradicts our original expectations that there would be an optimal frequency at which to breathe during fires.

This in-depth model of tracheal burns allows physicians to understand burn patterns in order to better target treatment. Knowing where the burns are located could allow for more directed and less invasive techniques. Additionally, we demonstrated that there are no preventative breathing techniques for when one is in a fire. As a consequence, more effort should be concentrated on treatment of the resulting burns.

2. INTRODUCTION

2.1 Background

The trachea is the main conducting airway of the body and as shown in Figure 1, allows the passage of air into the bronchi and eventually to the lungs. It is composed of three distinct layers: the mucous membrane, which traps inhaled foreign particles and moisturizes inhaled air; the connective tissue which is composed of smooth muscle that contracts and expands in response to environmental stimuli; and the cartilaginous C-rings, which provide rigidity and prevent the trachea from collapsing (Figure 2) [2]. Mechanically, the trachea functions to resist pressures during inspiration and expiration. Biologically, it acts as an air filtration system to prevent foreign matter from getting into the lungs [4]. Hot air burns the connective tissue in the trachea and significantly alters its mechanical and biological functions [10].

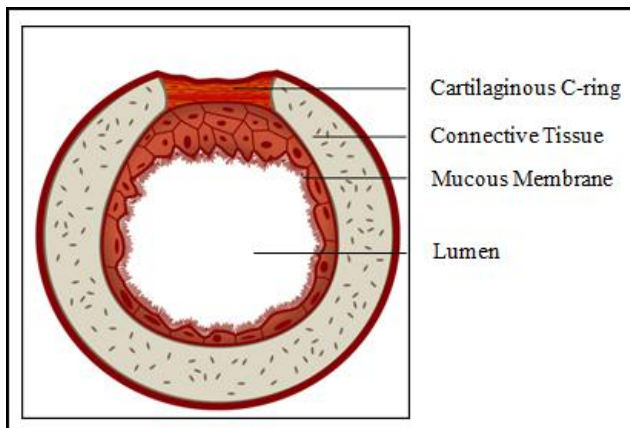


Figure 2. Cross Section of trachea

Hot air is convected through the lumen of the trachea heat after which heat is conducted into the connective tissue and Cartilaginous C-ring of the trachea.¹⁰

in which only the outer layer of tissue is burned. Second degree burns are those where the first layer of tissue is burned through. Second degree burns cause the development of blisters as well as severe pain and swelling. Third degree burns, the most serious burns, involve all the layers of the tissue and cause permanent damage. Areas of third degree burn are often charred black or appear dry and white [8].

The mucous lining of the trachea unexpectedly reduces the extent of burn damage by the

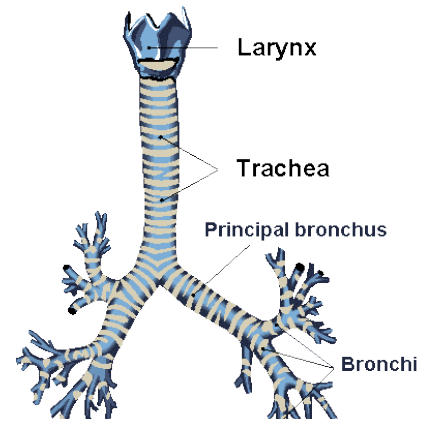


Figure 1. Image of trachea

Air flows into the mouth past the larynx through the trachea, into the bronchi, and then eventually to the lungs.⁹

Tracheal burn is caused by two primary factors; the convection of hot air through the lumen of the trachea followed by the conduction of heat through the connective tissue (Figure 2). As the hot air flows into the trachea, a temperature gradient develops between the lumen and deeper tissue and heat flows into the connective tissue. The increase in temperature of the connective tissue above a given threshold temperature induces first, second, and possibly third degree burns to the trachea. In humans, this threshold temperature is 45°C [13]. First degree burns, which are the least serious, are those

evaporation of moisture from the saturated mucous membrane. Evaporating water transports energy away from the tissue, energy that would otherwise be conducted into the tissue and contribute to the severity of the burn[13].

Recent advances in burn care techniques, such as fluid resuscitation formulas, have contributed to a decrease in burn mortality [13]. However, most of these advances are treatment techniques and few measures are available to reduce or even prevent burn injury at the time of hot air inhalation. In order to better understand the effects of burn damage on the trachea, improved knowledge of the heat transfer through the trachea is important. By establishing a quantitative model of the burn damage, it may be easier to dictate a definitive method for breathing when encountering hot gases in order to minimize damage.

We modeled the heat transfer in the connective tissue of the trachea in COMSOL finite element software. The model contains two governing equations—heat transfer through the connective tissue of the trachea, and the burning of the connective tissue, specified using a chemical reaction that follows first order kinetics. The heat transfer equation modeled the temperature gradient established by the hot air boundary condition. The convective heat transfer coefficient at the inner surface of the trachea depends on various properties of the flow field, including breath frequency and velocity of inhaled air. The burn equation uses the Arrhenius equation, in which the rate constants depend on the temperature solutions obtained from the heat equation.

2.2 Design Objectives

The goal of the project was to develop a model of the process of tracheal burning. Since the model is quantitative in nature, our results were highly dependent on numerous simplifications and high levels of uncertainty in geometric and material property data. Additionally, quantitative data has little practical value because no realistic accident scenario will match the model precisely. Our focus was therefore on qualitative relationships and trends, which we outline below.

We developed the model with enough detail to provide some insight into the following design objectives:

1. Determine how environmental factors such as external temperature and length of exposure affect both the severity and the spatial distribution of burn in the trachea.
2. Determine how the frequency and tidal volume of an individual's breath cycle affect the severity of a tracheal burn after a given period of time.
3. Determine an optimal breathing strategy that minimizes the extent of the burn damage in the trachea but maintains a constant average rate of respiration

2.3 Model Design and Schematic

The following section outlines the assumptions required to mathematically describe the physical processes of heat transfer to the trachea from inhaled air, heat conduction through the tissue, and the subsequent burning of that tissue. We begin with a discussion of the meaning of the types of tissues in figure 2 in the context of heat transfer, arriving at the decision to neglect their distinctions as well as the contribution of the mucus membrane to evaporative cooling. Next, we develop a model for the heat transfer characteristics of the fluid phase of the problem. This model captures the relationship between simple, meaningful data on breathing to heat transfer at the tracheal wall. Finally, we discuss a kinetic model that couples heat transfer to the extent of tissue damage, our ultimate variable of interest. Our discussion throughout this section is qualitative; a precise mathematical problem statement is presented in appendix A.

In order to accomplish our design objectives, we chose to model only the connective tissue of the trachea. Initially, we had thought to include both the cartilaginous rings and mucous membrane of the structure. However, further analysis determined that the burn only permeates slightly below the surface of the connective tissue and therefore does not reach the cartilaginous portion of the trachea. The mucous membrane, which we had initially thought would reduce the severity of the burn by transporting heat away from the connective tissue, proposed many implementation problems in COMSOL. To implement the evaporation from the tracheal wall, we required the rate of evaporation from the surface of the tissue, which in turn required that we solve for the concentration gradient of water vapor in the inhaled air. By multiplying the mass transfer coefficient by the concentration gradient between the dry inhaled air and the saturated mucous membrane and by the heat of evaporation, we obtained the rate of evaporation from the trachea. This was then modeled as a negative source term in the heat equation. Unfortunately, when we implemented this in COMSOL, the heat loss from the evaporation of the fluid overpowered the heat gain from the hot air inhalation and showed that the trachea was cooling down. This may have resulted from the assumption of *dry* (zero moisture) inhaled air, which made the concentration gradient very large. However, increasing this concentration (to greater than zero), still showed the heat loss from evaporation to be greater than the heat gained from conduction. Thus, we assumed the trachea to simply be a hollow cylinder consisting only of connective tissue. In COMSOL, we modeled this as a 2-dimensional axis-symmetry geometry in cylindrical coordinates.

Inhaled air is the ultimate source of energy driving the burning processes, and thus the convective heat transfer from the air to the tracheal wall is an essential aspect of the physics of this problem. Constructing a detailed model of airflow in the trachea would require a high level of geometric detail and a precise description of the human breath cycle and represent a departure from the scope and goals of our project. Furthermore, such a model would require extending the boundaries of the model to a location where the flow field is known and may be prescribed as a boundary condition. Specifically, the development of flow through the nostrils and the nasal cavity is non-trivial, and we cannot precisely model the flow in the trachea without also

modeling the flow in these regions. We therefore developed a simplified model of the airflow that meets the project goals without overreaching the limitations imposed by the model's scope.

Exact flow conditions at the inlet and outlet of the trachea are unknown, but physiological data on the frequency of breaths and the volume of air inhaled per breath is readily available. These data determine the time dependence of the flow velocity averaged over the tracheal cross-section. Any periodic time dependence would capture the essence of the breath cycle; we adopted the sinusoidal dependence expressed in equation 7 in the appendix, which gives the cross-section averaged velocity as a function of time, parameterized in terms of the physically meaningful breath frequency, tidal volume, and cross-sectional area of the trachea. The Reynolds number based on diameter corresponding to the maximum mean velocity for standard physiological values of the parameters falls squarely within the laminar range, and motivates the following treatment of the flow as a spatially developing boundary layer problem.

As air flows through the trachea, the thicknesses of the viscous and thermal boundary layers increase with downstream distance from the inlet. The thickness of the boundary layer determined by the Blasius solution at the far end of the trachea is small compared to the diameter of the trachea, allowing curvature to be neglected in this problem. To this observation, we added a simplifying assumption about the time dependence of the flow field. Although the bulk velocity varies throughout the breathing cycle, we assumed that at any moment the boundary layer is nearly developed in time, but that this boundary layer corresponds to the instantaneous bulk velocity. These assumptions motivate the use of an experimental correlation giving the local heat transfer coefficient in terms of instantaneous bulk velocity and downstream distance (equations 4, 5, and 6).

The correlation given in equations 4, 5 and 6 gives the local heat transfer coefficient as a function of time and space. In general, it specifies that the heat transfer coefficient increases with downstream distance (increasing distance from the proximal end of the trachea during inhalation and increasing distance from the upstream end during exhalation) and increases and decreases throughout the breathing cycle to track corresponding increases and decreases in bulk airflow velocity. Errors in the heat transfer coefficient result from both the simplifying assumptions required to use this correlation and from errors in the values of the parameters used to quantify the flow field. It should be noted that similar errors would accompany the assumptions necessary to fully specify the boundary conditions in a transient flow field simulation.

Using the heat transfer coefficient, we used a convective heat transfer boundary condition for the left boundary of the connective tissue. For the right side of the connective tissue, we assumed that there is no temperature gradient far from the air flow, and thus a no flux boundary condition was used. We also assumed that there is no heat flux in the longitudinal direction of the trachea at the upper and lower boundaries and enforced insulated boundary conditions there accordingly. The initial temperature of the trachea was assumed to be at body temperature (310K).

A rich set of chemical and physical processes occur in burning tissue, but the focus of this study is on a physical setting for tissue burning rather than on the details of the process itself. We therefore adopted a simple but well-established kinetic model for the burn process that represents burn severity as the concentration of an abstract chemical species undergoing a 0th order chemical reaction [3,5]. This concentration, Ω , has arbitrary units and must be interpreted empirically. We assumed that the rate constant depends only on temperature, and that this dependence takes the form of the Arrhenius equation. We implemented the kinetic equation for Ω using COMSOL's general diffusion equation with diffusivity set to zero and with the source term set to the rate of reaction. All boundaries of the model were set to be insulated and the initial concentration of burn in the trachea was set to zero since there is initially no burn throughout the region.

The schematic and all boundary equations are shown in Figure 3 below (governing equations are discussed in Appendix B).

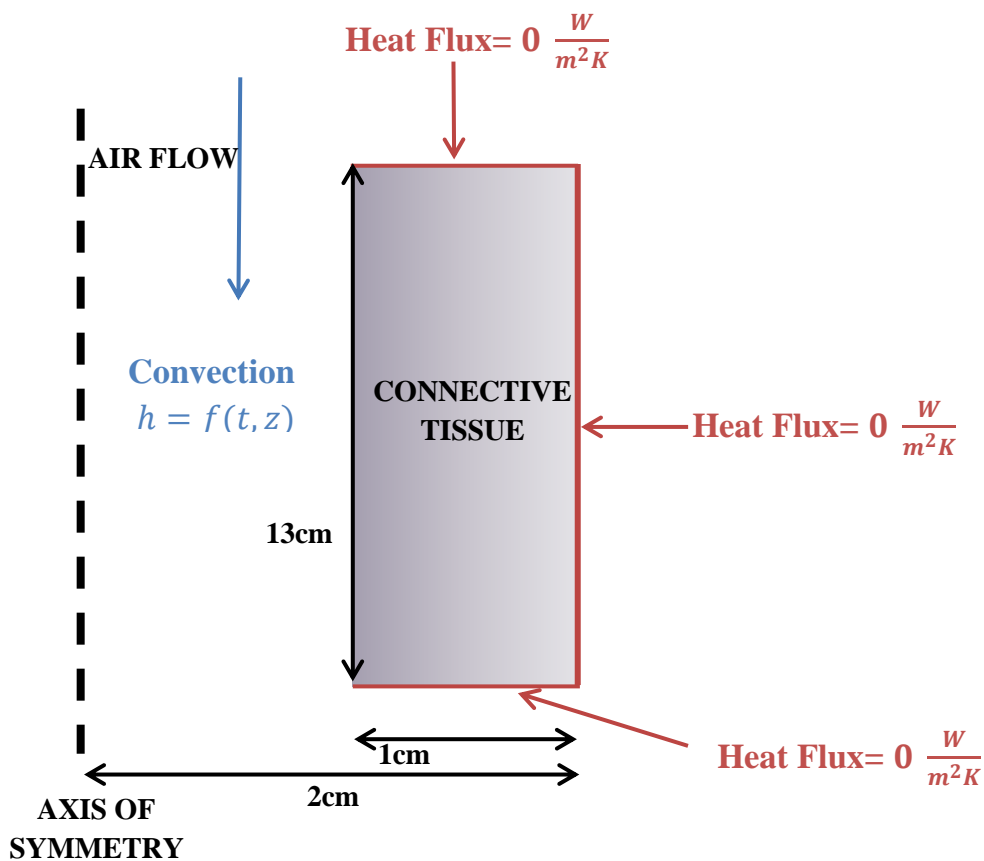


Figure 3. Schematic of the trachea with dimensions and boundary conditions. The top, right, and bottom surfaces were assumed to have zero heat flux, while the left boundary was set to a convective flux. The model is axisymmetric with the axis of symmetry shown.

Figure 3 shows the schematic for our model as implemented in COMSOL. For heat transfer, all boundaries except the inner wall were set to have a heat flux of zero. The inner wall had a convective heat flux boundary condition. The trachea itself was set to a width of 1 cm located at a distance of 1 cm from the axis of symmetry. In the z-direction, the trachea was set to be 13 cm long. For the burn concentration physics, all boundaries had a flux of zero.

3. RESULTS AND DISCUSSION

3.1 Solution Analysis

Although the model developed in the preceding section retains only the essential details of the physical process under consideration, it has enough flexibility to investigate our design goals. Each of these objectives seeks to determine how one aspect of a burn situation affects the severity of the burn. We refine this general and physically meaningful formulation into a mathematical question about how changes in one of the model's parameters affect definite characteristics of the model's solution. Such a statement, thus formulated, motivates several series of simulations. In each series, one parameter under study is varied over a range of values and the simulation is repeated for each value. The results of the simulation, summarized succinctly as scalar statistics, are compared. Such comparison allows us to draw conclusions about how each parameter affects burn severity.

Results Overview: Contour Plots of Temperature and Burn Severity

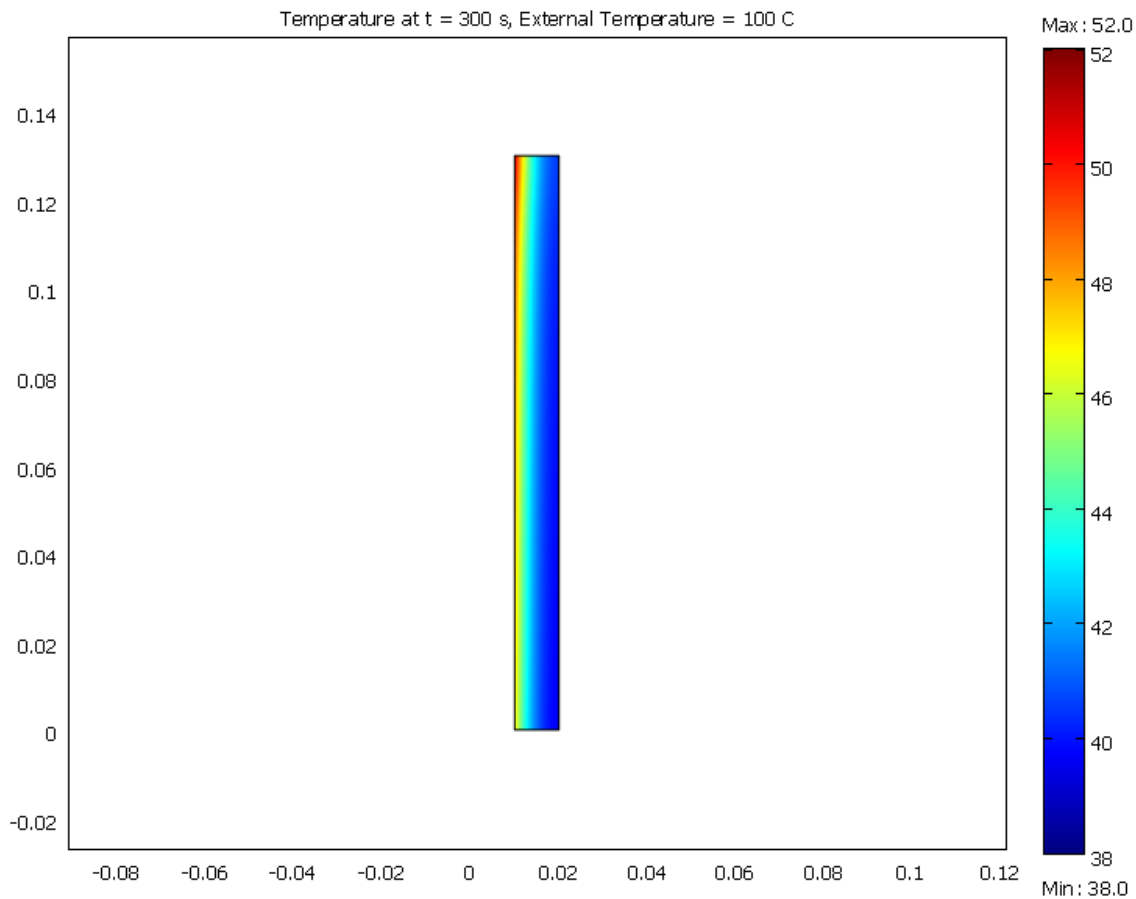


Figure 4. Contour Plot of Temperature at 5 minutes. The temperature is largest at the proximal end of the trachea, where the hot air enters. The air cools as heat is conducted into the trachea, so the distal end heats less. In addition, the temperature peaks at the inner wall and decrease radially.

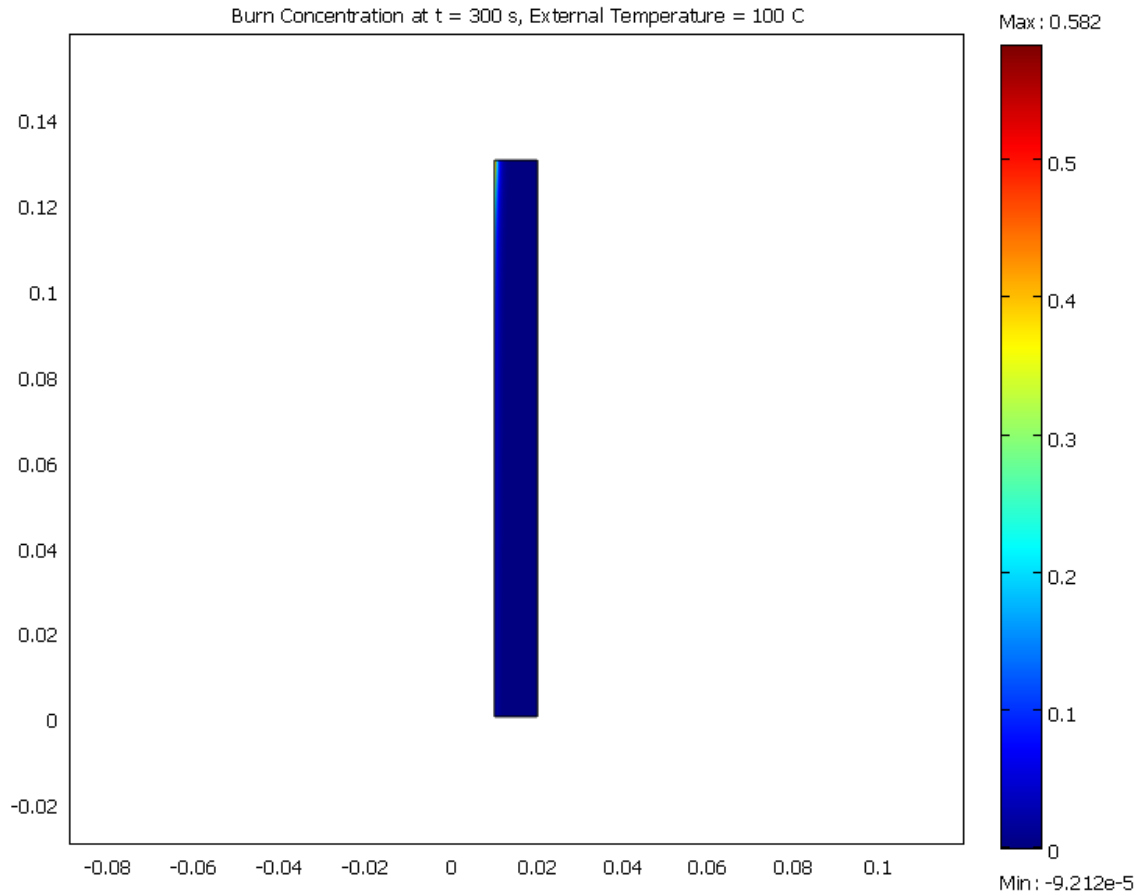


Figure 5. Contour Plot of Burn at 5 minutes. The burn occurs predominantly at the proximal end of the inner wall of the trachea. The burned portion of the trachea is relatively small as most of the trachea remains below threshold temperature.

Figure 4 and 5 show the temperature and burn contour respectively at the end of 5 minutes, at an external air temperature of 100C. As shown in Figure 4, the temperature is largest at the proximal end of the trachea, where the temperature of the incoming air is the largest, and decreases along the length of the trachea, as the air cools. The temperature also decreases in the radial direction as heat is conducted deeper into the trachea.

Similarly, Figure 5 shows the largest concentration of burn at the proximal end of the trachea. According to Arrhenius equation, the concentration of burn is only a function of time and is constant at a given temperature. The burn only propagates a very small amount into the connective tissue of the trachea. As shown in Figure 5 above, a majority of the trachea remains at zero concentration of burn.

Design Objective 1: Effect of Environmental Factors

We conducted simulations examining the extent of burn for each of a range of external temperatures. A meaningful benchmark for burn severity provided by Henriques et al. is the value of Ω at which 1st degree burn is sustained [7]. Regions of tissue for which Ω is greater than this threshold have sustained at least a 1st degree burn. As a means of summarizing the overall severity of the burn throughout the tissue domain, we calculated the volume of tissue that had sustained a 1st degree burn or higher using equation (11) and plotted this statistic over a 5 minute time interval for each external air temperature in Figure 4 below. For a given temperature, the total amount of burn remains at zero until the temperature in some part of the domain reaches the critical temperature (45°C) at which tissue damage begins. The burn reaction proceeds in this region, which expands as the heat transfer process evolves in time, and eventually the extent of burn in some region exceeds the empirical threshold corresponding to a 1st degree burn. The volume of this affected region continues to grow with time.

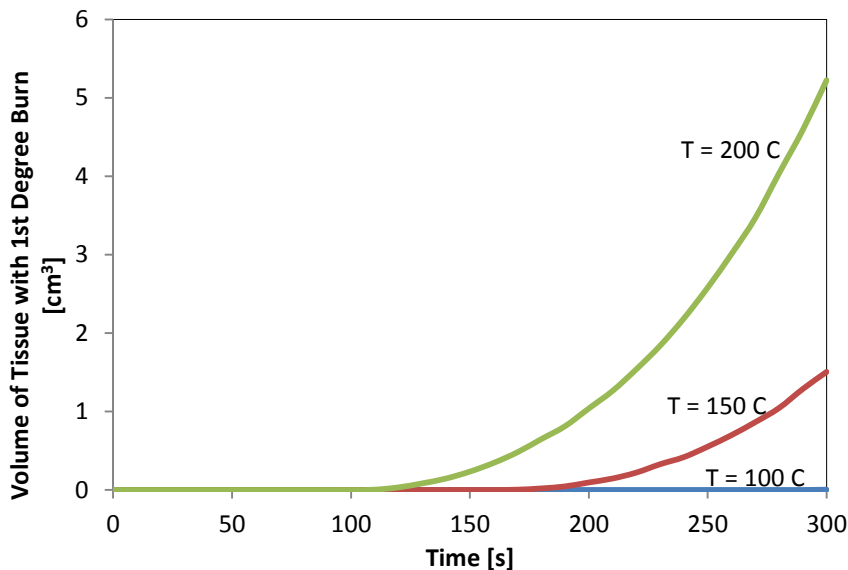


Figure 6. Effect of external air temperature on burn severity (volume of first degree burn). Variation of burn severity with time and with external temperature. Increasing temperature leads to a reduction in the time required to achieve 1st degree burn somewhere in the tissue, and an increase in the total volume of tissue affected by 1st degree burn at any given time.

As evidenced in Figure 6 above, increasing external air temperature accelerates the burning process and thus decreases the time required for a 1st degree burn to appear at some point in the trachea. From that time onward, an increase in temperature leads to an increase in the volume of tissue affected by burn.

We explore the effect of temperature on the spatial variation of burn intensity in Figure 5, which shows that the tracheal burns are more concentrated at the proximal end of the trachea, where the hot air enters.

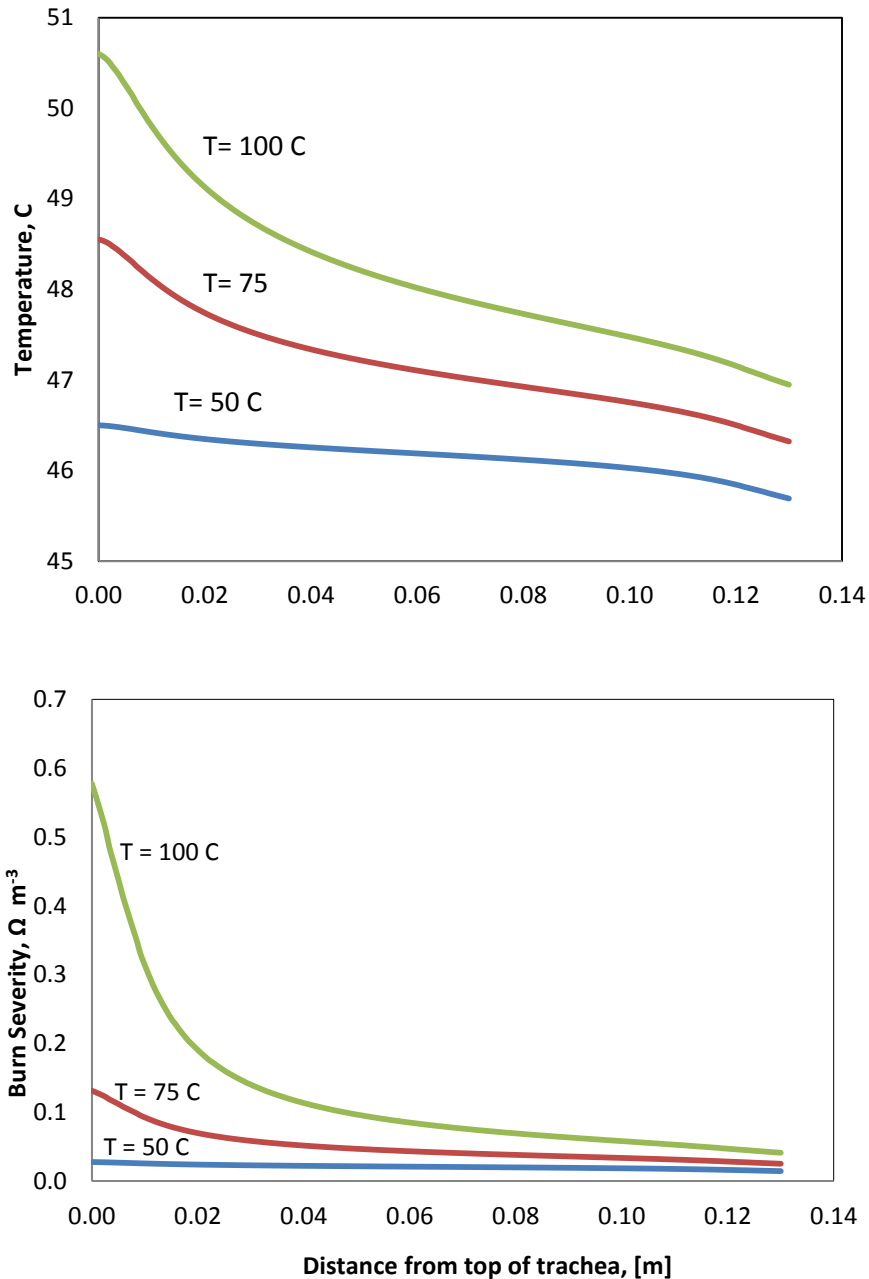


Figure 7. Effect of air temperature on burn severity and tissue temperature: spatial variation. Spatial variation of temperature and total burn are plotted for external air temperatures of 50, 75, and 100 C along the inner wall of the trachea. The left end of the graph corresponds to the mouth end of the trachea. Note the increase in spatial variation and in overall burn severity with increasing air temperature.

The temperature is the largest at the proximal end of the trachea, and decreases along the length of the trachea. This data fits with intuition that more burn will occur at the air inlet since the air will cool as it travels through the trachea. Furthermore, higher external air temperature leads to more dramatic spatial variation in burn intensity.

Design Objectives 2 and 3: Breathing Parameters on Burn Severity and Optimal Breathing Strategy

The rate of convective heat transfer at the tissue-air interface, and thus the extent of burn damage in the tissue, depends on both the amplitude and temporal frequency of the bulk velocity of the inhaled air. These quantities are directly related to the tidal volume and the breathing frequency, which an individual exposed to a fire could control consciously in an effort to minimize burn damage. We therefore explore the effect of varying breath frequency and amplitude on the extent of burn damage.

An individual does not have the freedom to adjust his or her breathing amplitude and frequency independently, as these two parameters together control the total rate of respiration. From the perspective of minimizing burn damage, reducing both amplitude and frequency makes sense, but in the limiting case this behavior is equivalent to holding one's breath. Frequency and amplitude are therefore constrained by the need to maintain some level of respiration. This consideration constrains the two parameter optimization space (amplitude and frequency) to a one-dimension space consisting of those combinations of amplitude and frequency that yield the same level of respiration. Determining the exact nature of the relationship between breathing frequency and tidal volume and the rate of gas transport in the lungs is beyond the scope of the present research. However, the rate of gas transport is at least loosely correlated to the average flow rate of air into the lungs. This motivates the following constraint

$$Q = \omega * TV = constant$$

In this equation, Q is the mean flow rate of air to the lungs to be constrained, ω is the breath frequency, and TV is the tidal volume, or total volume of air inhaled during one breath. Figure 6 shows the combinations of frequency and tidal volume used in this analysis, all of which lead to the baseline level of respiration.

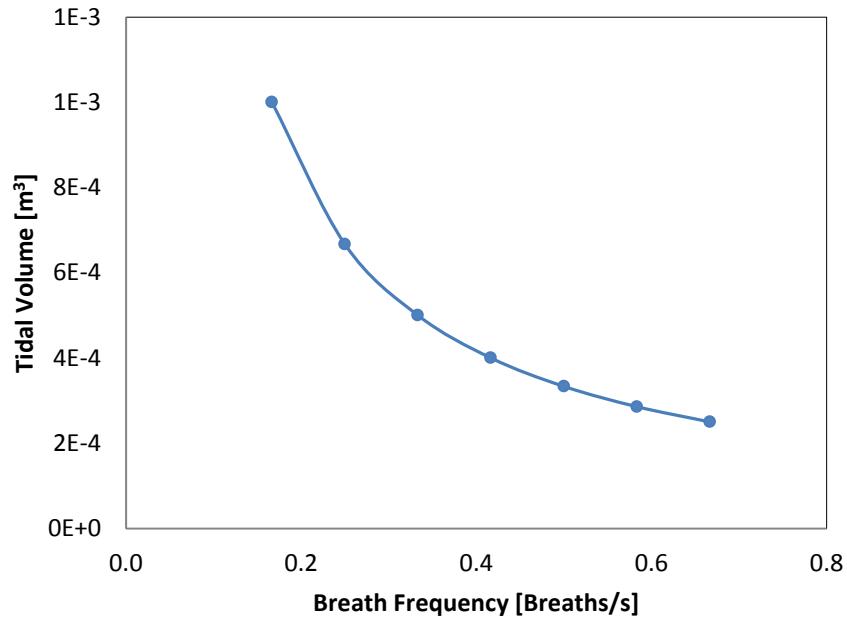


Figure 8. Sampled Breathing Parameters, constant respiration rate. This figure shows the tidal volume necessary to keep respiration rate constant when breathing frequency is varied. The points shown are those chosen in our analysis of the effect of these parameters on the extent of burn in the trachea.

We conducted a simulation for each set of values and calculated the volume of tissue with 1st degree burn after 5 minutes. These data are plotted in Figure 8. Figure 8 shows the tidal volume necessary to keep respiration rate constant when breathing frequency is varied. The points shown are those that were chosen in our analysis to determine the effect of these parameters on the extent of burn in the trachea.

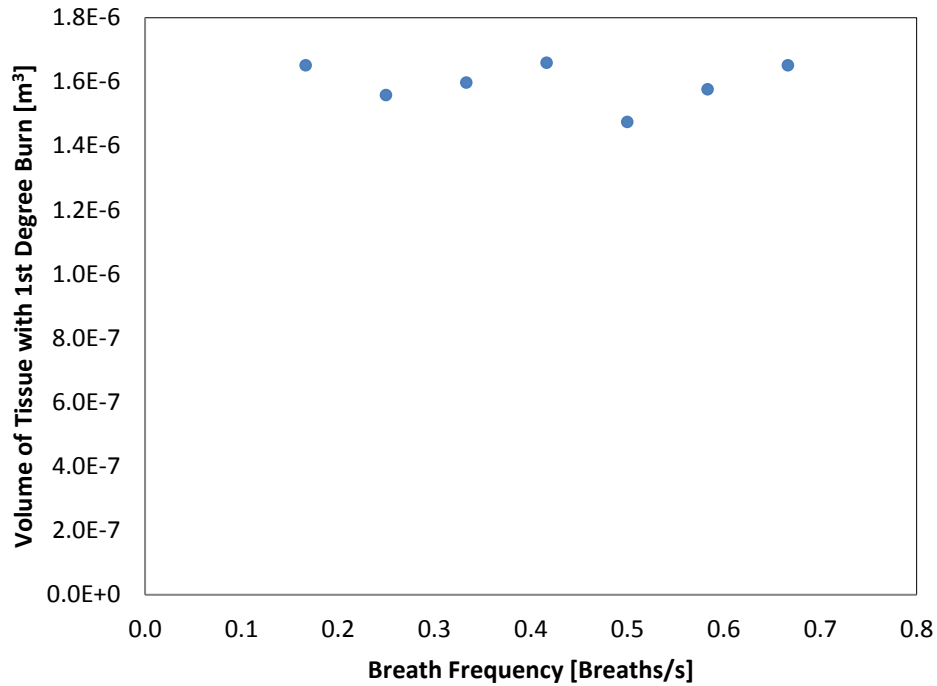


Figure 9. Variation in burn severity with breath frequency at constant respiration rate. Breath frequency has a small relative effect on burn severity when total respiration rate is constrained.

As evidenced in Figure 9, there is no obvious correlation between frequency and burn severity when the overall rate of respiration is constrained.

To examine the effect of reducing or increasing the total respiration rate, we hold the tidal volume fixed and adjust the frequency. Simulations for this set of parameter values examine the reduction in burn that may be realized by depressing total respiration rate. The results are plotted in Figure 8.

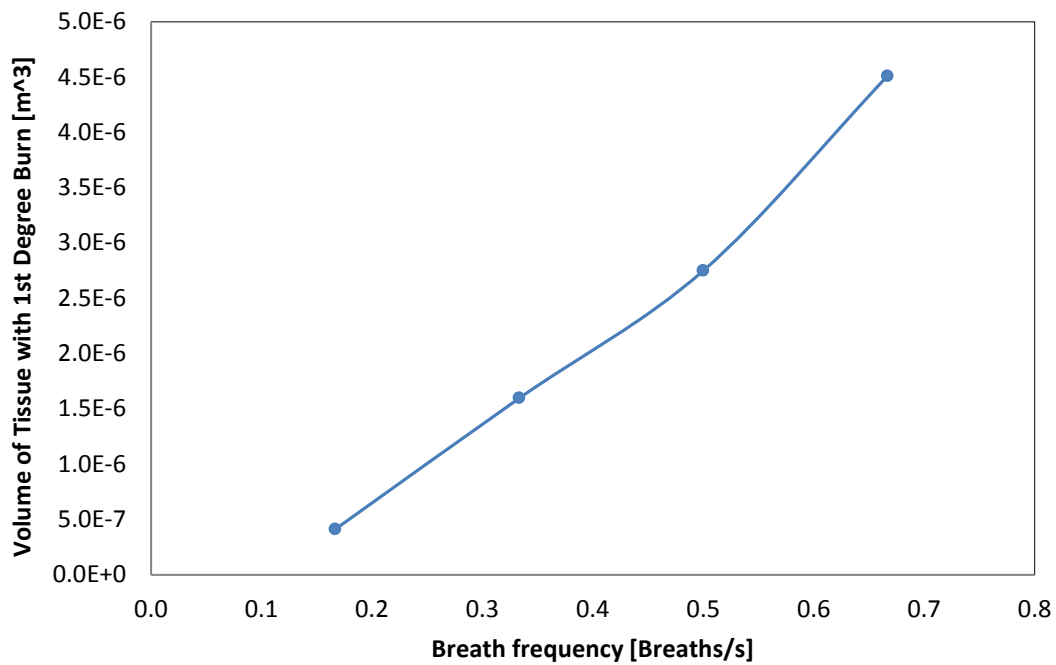


Figure 10. Burn Severity after 300s for varying breath frequency at variable respiration rate. Increasing breath frequency without adjusting breath volume leads to a higher overall respiration rate and a higher mean flow velocity with air temperature at 150°C. This contributes to a higher heat transfer coefficient and a more severe burn at any given time.

As Figure 10 shows, increasing breathing frequency at constant tidal volume leads to a marked increase in burn severity. The data is consistent with the physically intuitive fact that at zero breath frequency, no burn is sustained.

3.2 Sensitivity Analysis

We concentrated our sensitivity analysis on the tracheal material properties and other parameters with the most uncertainty. We did not conduct analysis on properties of air, because their values are well known at a given temperatures.

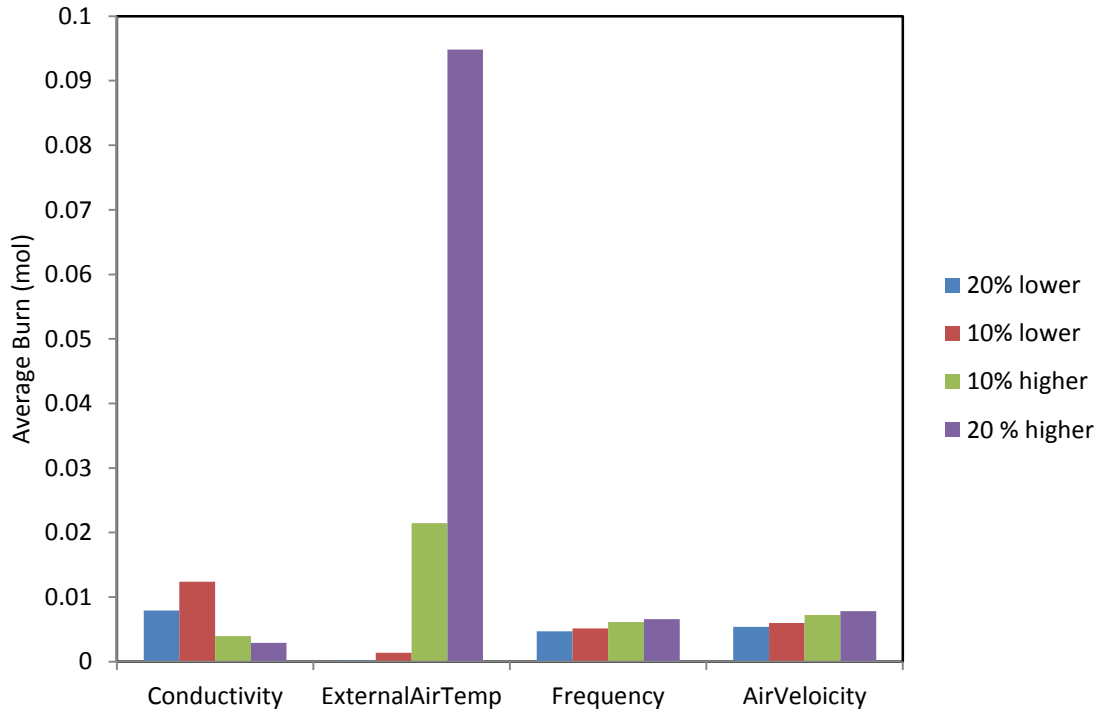


Figure 11. Sensitivity analysis. This shows variation of conductivity and the external air temperature. Conductivity, frequency, and air velocity have little effect on the average burn in the trachea, but external air temperature causes dramatic changes.

The four parameters that were varied in the model were the conductivity of the connective tissue, the temperature of the external air, the frequency of breathing, and the velocity of air at the inlet of the trachea. Each of the parameters was varied by 10% and 20% above and below the value used to generate the results. With these parameters, we calculated the average burn in the trachea to determine how these changes affected overall burn. As shown in Figure 9 above, the conductivity, breathing frequency, and air velocity all had a relatively insignificant effect on the average amount of burn in the trachea. On the other hand, external air temperature had a marked effect on the average amount of burn in the trachea. We can conclude that the inhaled air temperature plays the largest role in determining the extent to which the trachea is burned.

3.3 Accuracy Check

Due to the lack of published data on tracheal burning, a validation of our solution is limited to a check with an analytical solution. We simplified the model to the point where we could solve it analytically and compared the analytical solution to the computational solution. The simplified COMSOL model had a constant air flow velocity (and therefore a constant heat transfer coefficient). The simulation was run for 300 seconds (5 minutes).

To solve analytically, we simplified the problem even further to a steady state heat transfer in only the radial direction.

General Equation for analytical solution:

$$\frac{d}{dr} \left(r \frac{dT}{dr} \right) = 0$$

Boundary Conditions for analytical solution:

1. $T_{r=2cm} = 310K$
2. $h(T_{air} - T_{r=1cm}) = -k \left. \frac{dT}{dr} \right|_{r=1cm}$

The first boundary condition states that the temperature at the farther tracheal wall remains at body temperature, 310K. The second boundary condition states that the heat gained by convection at the inner tracheal wall is equal to the heat flux (via conduction) through the inner tracheal wall.

The analytical solution yields a temperature of 326K at the inner wall of the trachea, while using COMSOL, we obtained a value of 327.5K at the inner wall 2cm from the proximal end of the trachea.

It is important to note that the boundary conditions at the far end of the trachea were different for the analytical and simplified computational solution. In the computational solution, we used a zero flux boundary at the far end, while in the analytical solution we used a constant body temperature condition. Since we assumed the region to be semi-infinite, this did not affect our results for temperature at the wall of the trachea, the parameter we were checking.

The close agreement of 1) the analytical solution at steady state and 2) the numerical solution near steady state provides some confidence that COMSOL has correctly implemented the essential aspects of our model. This analysis does not confirm that the additional details of the full model have been implemented correctly, nor does it allow a comparison to the real physical process. Such an analysis would require experimental data currently unavailable in the literature.

4. CONCLUSION

Our model showed that increasing external air temperature increases both the total amount of burn in the trachea and the amount of burn at the proximal end. It was determined that while the respiration rate is kept constant (since we want the lungs to continue to receive the same amount of oxygen, this is the most physical) the amount of burn within the trachea does not change with increasing frequency. However, when the respiration rate is varied, the total amount of burn in the trachea increases with increasing breathing frequency. This makes sense intuitively, since in the limiting case of holding one's breath, there should not be any burn in the trachea. These results allow physicians to understand tracheal burn patterns in order to better target treatment. Knowing where the burns are located could allow for more directed and less invasive techniques. Due to the fact that there are no preventative breathing techniques for when one is in a fire, more effort should be concentrated on treatment of the resulting burns.

4.1 Realistic Constraints

In considering the realistic application of our model, we were concerned about the nasal cavity, specifically its function in preconditioning air. Humans breathe in through their nose and the nasal cavity guards the lung against invading particles. This cavity conditions the incoming ambient air to nearly body temperature. Naftali et al. has shown that during quiet breathing through the nose, ambient air at 20-25°C is conditioned up to 34°C [9]. Measurements even in a very cold environment of -18°C revealed heating of the inspired air to about 30°C. Another study found that air between -30°C and 50°C is generally conditioned to anywhere between 31°C and 37°C [3].

Although this data does not apply directly to our model, it demonstrates that preconditioning will decrease the ambient temperature before it reaches the trachea if it is too hot. Thus, the air flowing through the trachea is not at peak fire temperature. Modeling heat and mass transfer through the nasal cavity would require a completely separate project and was not included in our analysis. However, we can extrapolate the data from this paper to determine the level of preconditioning during fires. We plotted the data of external temperature versus temperature in the pharynx—the air after conditioning—and used a linear regression to fit a curve to these points (Figure C1 in Appendix C). We found that the flames in room fires reach average temperature of approximately 900°C [1]. Our equation demonstrates that the nasal passages would lower this temperature of this air to about 69°C once it reaches the trachea. In our analysis we chose to vary the inlet trachea temperature between 50°C and 100°C.

Our model attempted to incorporate the necessity of oxygen transport by examining the effects of breath frequency at a constant respiration rate. While this is more realistic than varying frequency at a variable respiration rate—which shows that the optimal breathing rate as no breathing at all—it still does not account for all the effects of gas transport in the lungs. A constant respiration rate does not imply constant oxygen transport in the lungs due to a varying

flow rate. It is a real possibility than any number of the breathing frequencies analyzed in the results would not provide sufficient oxygen transport in the alveoli.

Our model neglects the geometric details of the trachea on all spatial scales. Small irregularities on the surface of the tracheal wall affect the development of the thermal boundary layer in the flow over the tracheal surface and ultimately affect the rate of convective heat transfer. Larger scale geometric features, particularly at the transitions between the nasal cavity and the proximal end of the trachea, and the bronchioles and the distal ends of the trachea, have similarly important effects on heat transfer.

APPENDIX A: Mathematical Model

A1. Governing Equations

Energy Equation

Two dimensional Energy Conservation Equation in Cylindrical Coordinates (Heat Transfer Equation):

$$(1) \quad \rho C_p \frac{\partial T}{\partial t} = k \left(\frac{1}{r} \frac{\partial}{\partial r} \left(r \frac{\partial T}{\partial r} \right) + \frac{\partial^2 T}{\partial z^2} \right)$$

Burn Quantification

The degree of burn, Ω , due to the fire is given by the following equation developed by Henriques and Moritz (1947):

$$(2) \quad \frac{d\Omega}{dt} = 0, T < T_{threshold}$$

$$(3) \quad \frac{d\Omega}{dt} = A_0 e^{-E/(RT)}, T > T_{threshold}$$

$$T_{threshold} = 45C$$

Where A_0 is defined as the frequency factor, E is the activation energy, and R is the universal gas constant. This was implemented in COMSOL 3.5 via the diffusion equation application shown below.

$$\delta_{ts} \frac{dc}{dt} + \nabla \cdot (-D\nabla c) = R$$

Where D is 0, $\delta_{ts}=1$, and R is set to $A_0 e^{-\frac{E}{RT}}$.

Heat transfer coefficient at the air-trachea interface

Heat transfer coefficient:

$$(4) \quad h(x, t) = \frac{Nu k_{air}}{x}$$

$$(5) \quad Nu = 0.332 Re_x^{1/2} Pr^{1/3}$$

$$(6) \quad Re_x = \frac{|u_{\infty}(t)| x}{\eta}$$

where k_{air} , Pr , and η are the thermal conductivity, Prandtl number, and kinematic viscosity of air, respectively (evaluated at T_0 and assumed constant throughout the problem). The free stream air velocity, $u_\infty(t)$, changes periodically throughout the breath cycle. We model the fluctuations as

$$(7) \quad u_\infty = \frac{V_T}{A} \pi \omega \sin(2\pi \omega t)$$

Where V_T is the tidal volume, or the volume of one breath, A is the cross sectional area of the trachea, and ω is the breathing frequency in breaths per second. Note that the product of cross sectional area and the velocity integrated over one inhalation cycle ($0 < t < \frac{1}{2\omega}$) is equal to the tidal volume.

The heat transfer coefficient, thus modeled, is proportional to $\frac{1}{\sqrt{x}}$ and varies periodically with time.

A2. Boundary Conditions

BC1: Tracheal Wall

$$(8) \quad h(T - T_{burn}) = -k \frac{\partial T}{\partial r}$$

BC2: Top, Bottom, and Far Wall

$$(9) \quad -k \nabla T \cdot \hat{n} = 0 \text{ where } \hat{n} \text{ is the unit vector normal to the boundary.}$$

A3. Initial Conditions

$$(10) \quad T(r, 0) = T_0$$

A4. Interpretation of Burn Severity

Definition of 1st degree burn: $\Omega(\mathbf{r}, t) > 0.54$

Volume of tissue with 1st degree burn:

$$(11) \quad V^{1st}(t) = \iiint_{Tissue\ Domain} (\Omega(\mathbf{r}, t) > 0.54) dV$$

A5. Input Parameters

Name	Description	Expression	Units	Reference
η	kinematic viscosity of air	15.68×10^{-6}	m^2/s	[12]
ω	breathing frequency	1/3	breaths/s	[11]
V_T	tidal volume	5×10^{-4}	m^3/breath	[11]
k_{air}	thermal conductivity	0.027	W/mK	[12]
Pr	Prandtl number for air	0.711	-	[12]
ER	activation energy/R, burn	7.5×10^4	K	[5]
R	gas constant	8.314	J/kgK	[12]
A	cross sectional area of the trachea	$\pi (0.01)^2$	m^2	[11]
T_0	body temperature	310	K	
T_{burn}	external air temperature	373	K	
ρ	tissue density	1000	kg/m^3	[11]
C_p	tissue heat capacity	4000	J/kgK	[11]
A_0	pre-exponential kinetic constant for burn	3.1×10^{98}	kg/m^3	[5]

APPENDIX B: Solution Strategy

B1. COMSOL Specifications

This project used COMSOL Multiphysics with transient heat transfer by conduction and burning set as a concentration physics. We used the direct (UMFPACK) solver to solve the algebraic equations. The simulation was run for 300 seconds with a strict maximum time step of 0.1 seconds and an initial time step of 0.001 seconds. The relative and absolute tolerances for the temperature were 0.01 and 0.001 respectively.

B2. Mesh Convergence

Experience suggests that the choice of discretization affects the accuracy of the solution, and that the solution approaches a limiting value as the mesh is refined. To examine the effects of mesh refinement on our solution, and to select a degree of refinement that provides an appropriate balance between computational expense and accuracy, we define a mesh convergence parameter intended to summarize the solution (which consists of the values of several field variables at each point in the spatial domain at each moment in time) as a single scalar. Likewise, we summarize the quality of the discretization with a single parameter, the number of elements in the mesh. We calculate the parameter from the solution and plot the results, using average temperature in the trachea as our convergence parameter.

From initial simulations and from intuition, we expect greater temperature gradients near the surface at the proximal region of the trachea than in deeper tissue at the distal end. We therefore structure the mesh such that the density of elements increases towards the inlet and towards the surface of the trachea, as seen in Figure B1. The computational domain is a rectangle, and thus we use rectangular elements for efficiency.



Figure B1. Mesh grid for trachea model in COMSOL

A single representative measure of the entire solution was defined as the temperature at point (0.011cm, 0.125cm). This statistic was determined for simulations run with different degrees of mesh refinement in an attempt to select an appropriate degree of domain refinement. A plot of the temperature at this point as a function of the number of elements can be seen in Figure B2.

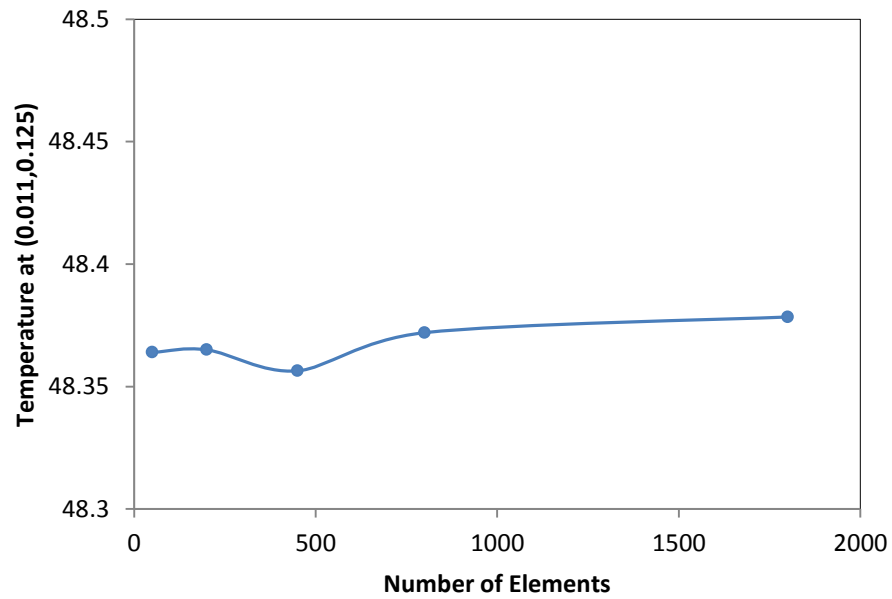


Figure B2. Mesh convergence for temperature at point (0.011cm, 0.125cm). This figure shows that the temperature at this point reaches a steady value after 800 elements.

The mesh convergence plot is seen in Figure B2. The solution appears to converge after 800 elements.

APPENDIX C: ADDITIONAL FIGURES

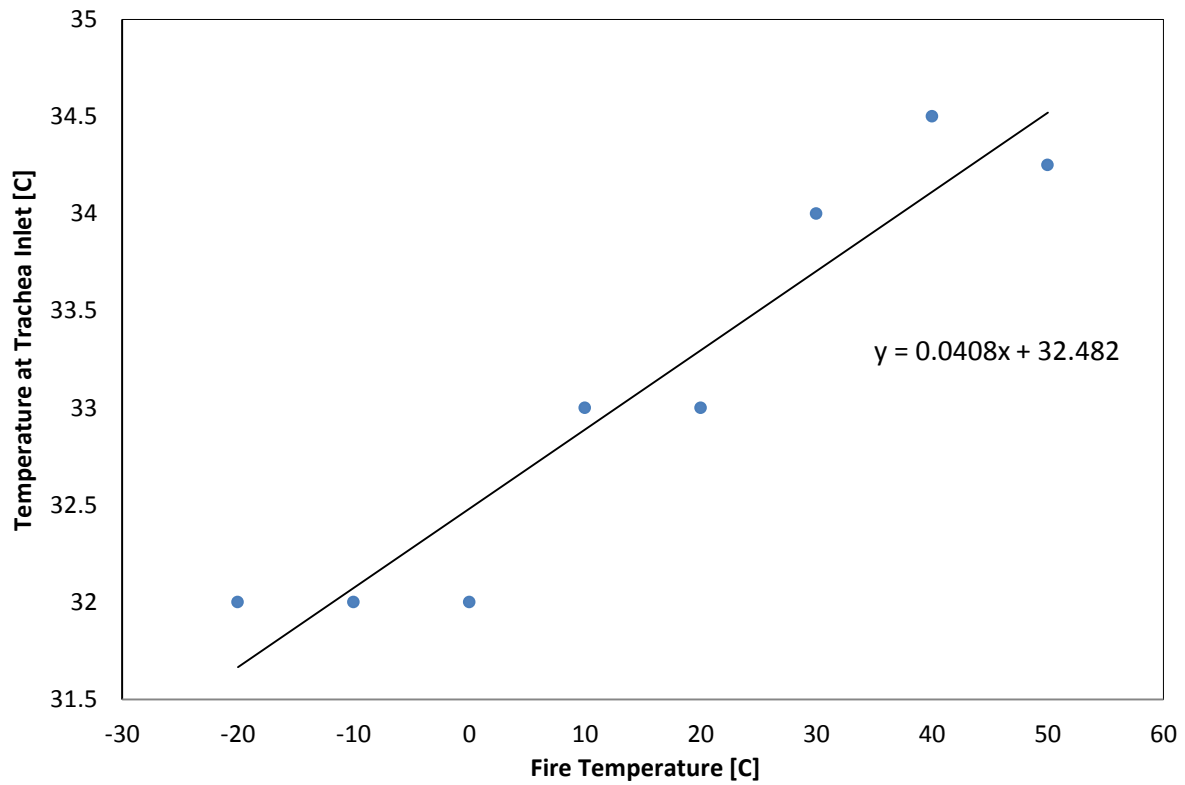


Figure C1. Tracheal Inlet Temperature as a function of Fire Temperature. According to Cole, temperature of the air at the pharynx is linearly proportional to the fire temperature at a relative humidity of 0% [3].

APPENDIX D: REFERENCES

1. Babrauskas, V. Temperatures in fires and flames. (25 Feb 2006). Visited May 8 2012. <<http://www.doctorfire.com/flametmp.html>>
2. Begis, D., Delpuech, C., Le Tallec, P., Loth, L., Thiriet, M., Vidrascu, M. A finite-element model of tracheal collapse. *Journal of Applied Physiology*, 64: 1359–1368, 1988.
3. Cole, P. Further consideration on the conditioning of respiratory air. *Journal of Laryngology and Otology*. 67:669–681, 1953.
4. Constantino M.L., Bagnoli P, Dini G, Fiore G.B: A numerical and experimental study of compliance and collapsibility of preterm lamb tracheae. *Journal of Biomechanics*, 37:1837-1847, 2004.
5. Datta, Ashim and Vineet Rakesh. *An Introduction to Modeling of Transport Processes*. Cambridge; Cambridge University Press, 2010.
6. Hanna, N.M., Jung, W.J. Optical Coherence Tomography Evaluation of Tracheal Inflammation. *RTO-MP-FHM-109*: 1-12, 2006.
7. Henriques, F.C., and Mortiz, A.R. Studies of Thermal Injury I. *American Journal of Pathology*, 23: 531-549, 1983.
8. MayoClinic. Burns: First Aid. Visited May 1 2012. <<http://www.mayoclinic.com/health/first-aid-burns/FA00022>>
9. Naftali S., Rosenfeld M., Wolf D.E. The air-conditioning capacity of the human nose. *Annals of Biomedical Engineering*, 33: 454-533, 2005.
10. Pruitt B.A., Goodwin C.W., Mason A.D. *Epidemiological, Demographic and Outcome Characteristics of burn Injuries*. London; Saunders Company, 1996.
11. Trachea Image. Visited Apr 3 2012. <<http://www.naturalhealthschool.com/img/trachea.gif>>
12. Trachea Cross Section Image. Visited Apr 3 2012. <http://www.promocell.com/fileadmin/promocell/Kapitelbilder/HumanTrachealSmoothMuscleCells_2.jpg>
13. Yong Gang L., Zhang J. Liu J. Theoretical evaluation of burns to the human respiratory tract due to inhalation of hat gas in the early stage of fire. *Burn*, 32: 436-446, 2006.

14. Yunus A., Çengel, and Michael A. *Thermodynamics: An Engineering Approach*. Boston: McGraw-Hill, 2001